Iraqi Geological Journal

Journal homepage: https://www.igj-iraq.org

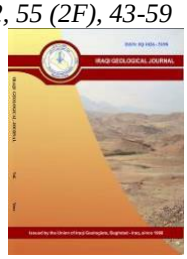

Geochemistry, Depositional Environment, and Provenance of the Cretaceous Radiolarian Chert in Northeastern Kurdistan, Iraq

Ruaa M. Al-Sheraefy[1,*], Falah M. Ahmed[2] and Mohamed A. Alrashedi[3]

[1] College of Sciences, University of Mosul, Mosul, Iraq
[2] College of Engineering, University of Kirkuk, Kirkuk, Iraq
[3] College of Petroleum & Mining Engineering, University of Mosul, Mosul, Iraq
* **Correspondence**: : roaamohmmed@uomosul.edu.iq

Received:
10 June 2022

Accepted:
23 August 2022

Published:
31 December 2022

Abstract

The radiolarian chert rocks are one of the most important indications of the existence of ophiolites because they are a source of silica supply. These rocks have been studied to refute and reject the idea that ophiolites do not existed. The Si/(Si+Al+Fe+Ca) ratio in the radiolarian chert indicates that the silica is of biogenic origin and adds SiO_2 from the shale fraction through diagenetic processes. The high values of Fe_2O_3 content indicate the hydrothermal effect during precipitation. This effect is controlled by the distance between the sediments and the mid-oceanic ridge or sea floor metamorphism. The phosphorus could be a direct result of volcanic activity associated with ophiolitic rocks, whereas, the negative correlation coefficient of phosphorous with calcium (r = -0.53) supports the idea that the source of phosphorous is volcanic activity that is not related to the carbonate fluorapatite mineral. REEs shows a basic difference as a positive cerium anomaly in section Q2 and a negative cerium anomaly in section Q1. The Al-Fe-Mn diagram shows that all samples fall into the field I non-hydrothermal zone, but in the SiO_2 vs Al_2O_3 diagram the samples of the Q1 section fall into the hydrothermal field, and samples of the Q2 section fall into the non-hydrothermal field. The input materials in Qulqula radiolarian chert come from terrigenous sediments in both sections. On the other hand, the Al/(Al+Fe+Mn) ratio range, (between 0.61 to 0.70), is very close to the average shale composite value, (0.6.19), which may reflect the contribution from continental and non-hydrothermal sediments, while the lower values of this ratio reflect hydrothermal source input. The MnO_2 /TiO_2 ratios ranged between 0.06 to 2.37 in section Q1 which represents typical characteristics of the deep ocean, trenches, and basaltic plateau sediments.

Keywords: Qulqula Formation; Radiolarian chert; Geochemistry; Provenance; Depositional environment

1. Introduction

The Qulqula Radiolarian Formation (QRF) is located in the Iraqi segment of the Zagros Folded and Thrust Zone (ZFTZ) in north-eastern Iraq close to the borders of Iran. The North Zagros Thrust Zone (NZTZ) forms the northeast boundary of a wide region of deformation within the Zagros Fold Zone (ZFZ). These zones are collectively referred to as the Zagros Fold-and-Thrust Belt (ZFTB). According to Bellen et al. (1959), (QRF) was first described by Bolton (1955), but a more precise definition and

DOI: 0.46717/igj.55.2F.3ms-2022-12-18

description were given by Bolton (1958). He mentioned that it consists of thick successions of bedded chert, shale, and siliceous limestone. In the field, the parautochthonous formation of Qulqula is strongly deformed and accreted on the autochthon platform carbonate (Balambo, Albian-Cenomanian) (Aswad,1999). The age of the Qulqula in the Iraqi segment, however, is controversial and has not yet been precisely determined, it ranges in age from Triassic to Cretaceous (Buday, 1980 Jassim, and Goff, 2006). Karim et al. (2009), noted that the lower part of the Qulqula formation is enriched in limestone rocks and interbedded with layers of radiolarian chert. Furthermore, in the Iranian terrane, Qulqula refers to the Kermanshah radiolarites terrane (Ali et al., 2014). The latter was recently dated using radiolarian biostratigraphy producing an age range early Pliensbachian stage to the Turonian stage for the youngest (Gharib and De Wever, 2010). The sampling procedure is rather difficult because the Iraqi segment stated above is highly deformed where fracture, fault, and fold can be recognized in the field. Furthermore, the location contains unexploded landmines. Accordingly, sampling is restricted to the alignment of the main road, Due to these restrictions, two sections were chosen for this study very carefully. These two sections contain different fauna, and this means that the 2 sections have different ages, as well as different provenance. The main objective of this study is determining the provenance and depositional environment of the Qulqula Formation based on geochemistry analysis and how these rocks are affected by the tectonic setting and volcanic activities.

2. Geological Setting

The studied area is located in Sulaimaniyah city, NE of Iraq, near the border with Iran (Fig. 1). The samples were collected from Qulqula Formation in two different sections, six samples from the first section symbolize (Q1) near Dolasur village, mainly forming of radiolarian chert. It should be noted that the aforementioned section is located above the Balambo Formation pointed by latitudes (35º 31" 00.24' N) and longitudes (45º 52" 40.50' E) (Fig. 1). The sequence stratigraphy composed of red clay beds overlapped with deformed beds of radiolarian chert colored reddish to brown (Fig. 2: a, b, c, d). Six samples were collected in the second section and symbolize (Q2) that located near the Nalparez village indicated by latitudes (35º 34" 48.24' N) and longitudes (45º 51" 37.68' E) as shown in (Fig. 1). An important field observation is a stratigraphic and lithologic difference between the two sections, where second section (Q2) consists of reddish siliceous clay and thinly bedded radiolarian chert with dark grayish shale as interstratified in carbonates rocks (Fig. 2: e, f, g, h). Briefly, the studied area is located within the Iraqi segment of ZFTZ which is referred to Qulqula-Khwarkurk subzone (Buday and Jassim, 1987). According to Aswad (1999), the Qulqula formation which is considered a terrane of oceanic affinity has accreted onto the Arabian shelf carbonates (autochthonous) during Late Cretaceous.

3. Materials and Methods

Twelve samples of radiolarian chert rocks were collected from two different sections of the Qulqula Formation in the Penjween area. The researchers were careful during collecting fresh samples after removing the surface layers that have been affected by weathering. The major oxides were analyzed in the whole rock. In addition, the analysis of trace elements and rare earth elements (REE), using Inductive Coupled Plasma-Mass Spectrometry (ICP-MS) in ACMA Laboratories, Canada after preparing the samples powder with a ring grinder. Thin sections were prepared in the workshop of the geology department / the University of Mosul. Optical microscopes were used in the laboratories of the Universities of Mosul and Kirkuk to study petrography.

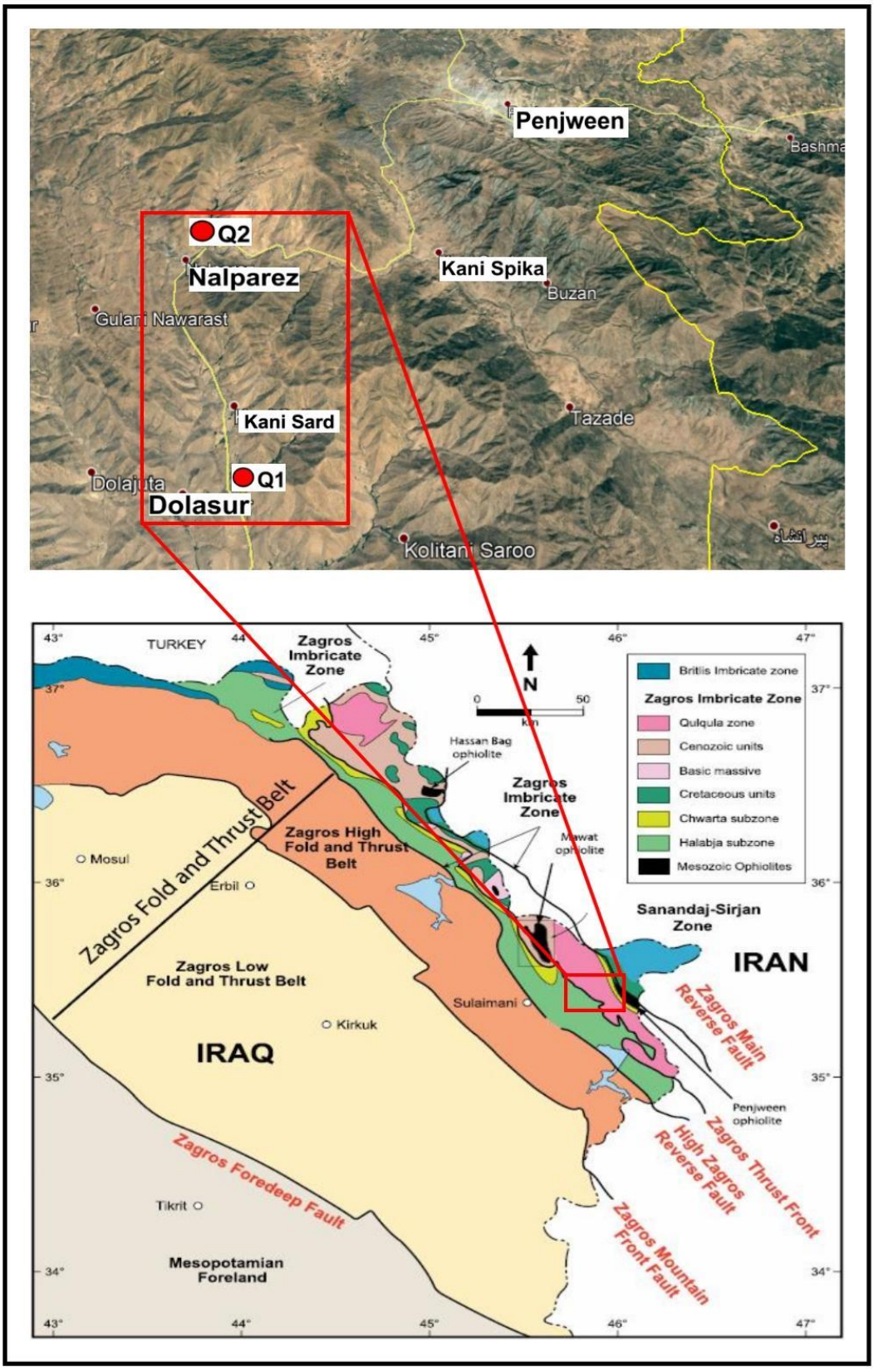

Fig. 1. Location of the study area and geological map of northeastern Iraq (modified after Al-Kadhimi et al., 1996)

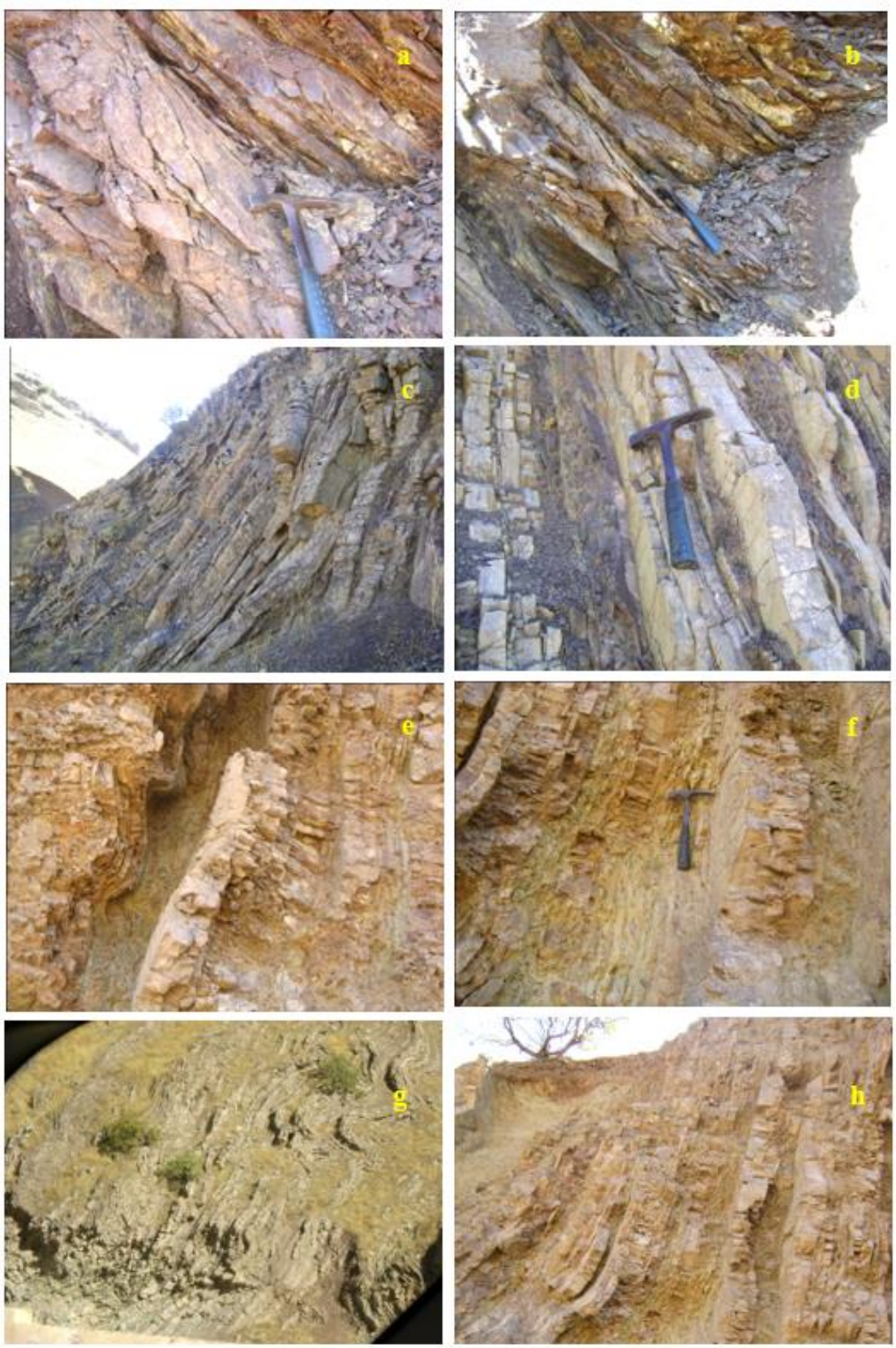

Fig. 2. Field photographs of the Qulqula Formation. (a, b, c, d) from Q1 section near Dolasur village. (e, f, g, h) from Q2 section near Nalparez village.

4. Results and Discussion

4.1. Petrography

Thin sections show many differences between the two sections of Qulqula Formation in color and fauna size. Section Q2 appears reddish and has larger and more numerous fauna consists of rounded remains of radiolarian skeletons (size ranges from 0.1 mm – 0.5 mm), and a few amount of micrite and sparry calcite as a matrix that formed cement materials (Fig. 3. a, b, c, and d), the reddish color reason may be due to the abundance of iron in the section Q2 samples (Table 1). Section Q1 contains small remains of radiolarian skeleton (size less than 0.2 mm) (Fig. 3. e, f) and enriched in micrite (lime mud) and a minor amount of sparry calcite that formed mudstone microfacies, sometimes limestones form interbeds within the radiolarian cherts or as thin lenses, fractures filled by calcite and recrystallized calcite are common (Fig. 3. g, h). The presence of micrite and sparite in the Q1 section is supported by chemical analysis that can be seen a high concentration of calcium carbonate (Table 1), these facies in section Q1 may be deposited in a low-energy environment. The effect of diagenesis processes in these facies is illustrated through the dissolution and cementation of micrite and sparite. The well-preserved radiolarian and the presence of several fauna types within the assemblages (taxa) are widely used for dating and determining the relative age of the radiolarian chert (Bragin et al., 2022). The difference in fauna and rock components of both sections reflects the different sedimentation environments, which will be discussed in detail later.

4.2. Geochemical Analyses

The major oxides, trace elements and REE for all samples are analyzed and listed in the Table 1, 2 and 5 in sequential. REE and some elements are normalized against chondrite (Ch), World Shale Average (Ave. Shale), Upper Continental Crust (UCC), Post Archean Australian Shale (PAAS), and North American Shale Composite (NASC). Silica was used as the denominator versus all variables.

Table 1. Geochemical analysis of major elements (wt %) in both sections

	Sample	SiO_2	TiO_2	Al_2O_3	FeO	MgO	CaO	Na_2O	K_2O	MnO	P_2O_5	LOI	Sum
Section Q1	Q11	83.30	0.24	4.16	1.93	0.78	6.45	0.17	0.80	0.03	0.07	0.08	98.01
	Q12	82.99	0.03	0.66	0.28	0.17	13.81	0.10	0.07	0.07	0.06	0.12	98.36
	Q13	81.46	0.08	1.68	0.84	0.41	14.16	0.11	0.25	0.08	0.03	0.13	99.23
	Q14	82.92	0.08	1.17	0.63	0.28	13.63	0.08	0.20	0.13	0.03	0.13	99.28
	Q15	93.71	0.03	0.42	0.17	0.07	5.11	0.07	0.07	0.05	0.01	0.05	99.76
	Q16	88.40	0.32	4.91	2.05	0.88	1.37	0.09	1.07	0.02	0.09	0.05	99.25
Section Q2	Q21	79.93	0.50	9.79	4.66	0.93	0.50	0.21	1.65	0.09	0.07	0.05	98.38
	Q22	79.49	0.63	10.86	5.02	1.04	0.48	0.29	2.11	0.04	0.09	0.06	100.11
	Q23	81.17	0.57	10.01	4.39	0.99	0.39	0.29	1.76	0.03	0.06	0.05	99.71
	Q24	81.18	0.52	9.83	4.35	0.90	0.42	0.22	1.84	0.02	0.05	0.05	99.38
	Q25	79.36	0.56	9.25	5.17	0.96	0.49	0.22	1.97	0.07	0.07	0.05	98.17
	Q26	80.03	0.54	10.25	5.03	1.01	0.39	0.29	2.02	0.05	0.06	0.04	99.71

LOI= Loss on Ignition

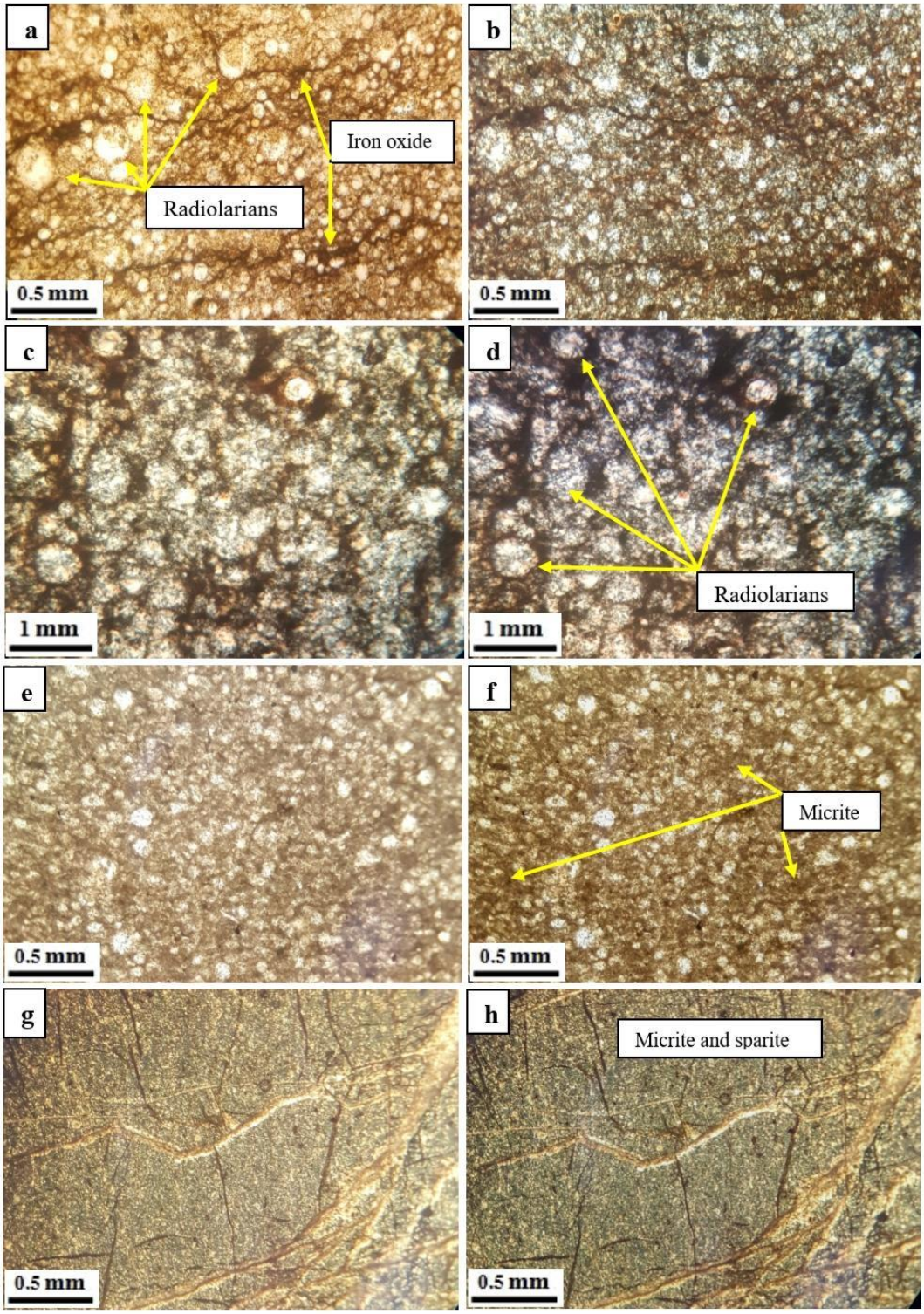

Fig. 3. Photomicrographs features of the Qulqula radiolarian chert: (a) Rounded radiolarians and iron oxide (PPL), b (XPL), (c) Large rounded radiolarian formed packstone (PPL), d (XPL) in Q2 samples, e (PPL), f) Small remains of radiolarian skeletons (XPL), g (PPL), h) Micrite and sparite (XPL) in Q1 samples, (PPL: Plain Polarized Light) and (XPL: Crossed Polarized Light)

Table 2. Geochemical data of trace elements (ppm) in both sections.

	Sample	Ba	Co	Cr	Hf	Ni	Rb	Sc	Sr	Th	U	V	Y	Zr
Section Q1	Q11	114.0	7.6	17.0	1.0	28.0	29.8	5.1	81.0	2.7	0.3	27.0	10.6	32.8
	Q12	17.0	12.7	1.0	0.1	5.1	2.6	1.2	84.0	0.6	0.3	5.0	10.3	5.3
	Q13	101.0	13.8	5.0	0.4	11.6	9.0	1.9	78.0	1.2	0.2	11.0	8.9	16.2
	Q14	94.0	12.9	5.0	0.3	12.5	7.3	1.8	102.0	0.8	0.6	13.0	6.3	10.3
	Q15	138.0	23.4	4.0	0.1	5.0	1.4	0.7	75.0	0.3	0.3	5.0	1.8	3.5
	Q16	101.0	8.3	22.0	1.2	20.5	37.3	7.8	39.0	3.1	0.5	45.0	10.3	45.3
Section Q2	Q21	108.0	32.1	52.0	1.6	62.5	61.5	10.1	108.0	7.7	1.0	82.0	14.9	63.8
	Q22	109.0	25.3	54.0	2.2	46.5	72.5	13.0	99.0	7.5	1.0	87.0	14.8	78.8
	Q23	93.0	23.4	45.0	2.2	51.8	64.5	11.2	88.0	7.3	1.0	110.0	11.8	72.9
	Q24	108.0	20.4	44.0	1.8	51.6	63.9	10.8	78.0	6.6	0.9	97.0	10.0	62.3
	Q25	101.0	21.8	48.0	1.6	49.6	64.4	11.6	93.0	6.8	0.9	99.0	12.5	65.6
	Q26	98.0	23.9	51.0	2.0	52.1	70.5	10.2	85.0	7.3	1.0	84.0	10.6	71.6

4.2.1. Major oxides

Silica. The SiO_2 is relatively high in all samples but varied in both sections. Silica content vary from 79.36% to 93.71% (Table 1). The Si/(Si+Al+Fe+Ca) ratio is used as an indicator for silica provenance in the radiolarian chert, this ratio in biogenic silica-rich sediments such as radiolarian chert has values ranging (from 0.8 – 0.9) (Ruitz-Ortiz et al., 1989). The values range in the Qulqula Formation range from 0.83 – 0.94 (Table 4).

Aluminum and titanium are related to aluminosilicates detritus minerals such as mica and clay minerals and may be a very good indicator for the terrigenous provenance materials (Rangin et al., 1981). The aluminum content is highly variable from 0.42 % to 10.86 % (Table 1), with an average concentration of 2.17 % in section Q1 which is much less than its concentration in section Q2 = 10%. Aluminum shows a high correlation coefficient ($r > 0.9$) with many major oxides such as titanium, iron, magnesium, sodium, and potassium (Table 3), which indicates their mutual source rock.

The TiO_2 values in the two sections range from 0.03 % to 0.63 %, high content is concentrated in section Q2. Titanium has a strong correlation with aluminum ($r = 0.99$), iron ($r = 0.99$), magnesium ($r = 0.94$), sodium ($r = 0.91$) and potassium ($r = 0.99$). This strong correlation may conclude that these elements are present within the same mineral, and it may be mica (sericite) or clay minerals. Sodium and potassium. The sodium content is relatively low in both sections, they range between 0.07 % to 0.29 % while potassium is higher in content and varies from 0.07 % to 2.11 % (Table 1). The strong correlation between Na_2O and K_2O and their very good correlation to most major elements like aluminum, titanium, iron, and magnesium as well as high values correlation coefficient to some trace elements such as chromium, hafnium, nickel, rubidium, thorium, uranium, vanadium, zirconium and total REE (Table 3) can be used as an indicator of the clastic phase for aluminosilicates minerals associated with chert (Murray et al., 1992). Iron and phosphorus. The high values of Fe_2O_3 content in radiolarian chert may indicate the hydrothermal effect during precipitation, this effect is controlled by the distance between the sediments and the mid-oceanic ridge (MOR) or sea floor metamorphism (SFM) (Halamic et al., 2005). Iron concentration is very variable in the two sections, its content in section Q1 ranges between 0.17 % and 1.93 %, while the content in section Q2 varies from 4.35 % to 5.17 %. Because of their assemblage in green clastic components such as altered volcanic rock fragments to chlorite and celadonite minerals, iron has a negative correlation coefficient to silica and calcium, a moderate correlation coefficient to loss on ignition, and a strong positive correlation to the other major

oxides except for manganese. The phosphorus, in the studied rocks- could originate from two different origins. Firstly, biogenic accumulated by bacteria from seawater as nodules or phosphatic sediment, and second origin, because of associated chert to ophiolitic rocks the phosphorus could be a direct result of volcanic activity and diagenetic processes in the sedimentation basin (Halamic et al., 2005). This may interpret the high phosphorous content in section Q2 as compared to section Q1. The P_2O_5 content in section Q1 does not exceed 0.048 on average while in section Q2 reached 0.065 % on average. The negative correlation coefficient of phosphorous with calcium (r = -0.53) supports the idea that the source of phosphorous is volcanic activity, not related to the carbonate fluorapatite mineral.

Table 3. Correlation coefficient [r] for major, trace elements and ∑REE, (Number of samples N= 12).

	SiO	TiO	Al₂O₃	FeO	MgO	CaO	Na₂O	K₂O	MnO	P₂O₅	LOI	Ba	Co	Cr	Hf	Ni	Rb	Sc	Sr	Th	U	V	Y	Zr	∑REE
SiO₂	1.00	-0.61	-0.63	-0.66	-0.59	0.16	-0.68	-0.61	-0.25	-0.37	-0.06	0.27	-0.29	-0.61	-0.59	-0.66	-0.61	-0.58	-0.60	-0.65	-0.60	-0.59	-0.78	-0.61	-0.73
TiO₂		1.00	0.99	0.99	0.94	-0.87	0.91	0.99	-0.33	0.62	-0.74	0.23	0.59	0.98	0.98	0.95	1.00	0.99	0.24	0.98	0.91	0.98	0.74	0.99	0.97
Al₂O₃			1.00	0.99	0.93	-0.86	0.93	0.99	-0.30	0.57	-0.72	0.23	0.63	0.99	0.98	0.97	1.00	0.98	0.28	1.00	0.92	0.97	0.74	0.99	0.99
FeO				1.00	0.92	-0.84	0.92	0.99	-0.23	0.55	-0.70	0.22	0.64	0.99	0.96	0.97	0.99	0.97	0.33	0.99	0.92	0.96	0.74	0.98	0.99
MgO					1.00	-0.82	0.84	0.94	-0.40	0.75	-0.66	0.25	0.36	0.91	0.95	0.89	0.95	0.95	0.07	0.91	0.78	0.89	0.79	0.96	0.90
CaO						1.00	-0.72	-0.87	0.54	-0.53	0.97	-0.46	-0.58	-0.87	-0.85	-0.81	-0.87	-0.87	0.04	-0.84	-0.76	-0.85	-0.46	-0.86	-0.78
Na₂O							1.00	0.91	-0.30	0.47	-0.60	0.12	0.60	0.91	0.94	0.89	0.92	0.88	0.38	0.93	0.85	0.89	0.69	0.92	0.94
K₂O								1.00	-0.33	0.60	-0.74	0.24	0.58	0.98	0.98	0.94	1.00	0.99	0.22	0.98	0.91	0.96	0.72	0.99	0.97
MnO									1.00	-0.45	0.60	-0.24	0.12	-0.24	-0.40	-0.18	-0.33	-0.36	0.63	-0.24	-0.03	-0.29	-0.09	-0.35	-0.20
P₂O₅										1.00	-0.40	-0.15	-0.06	0.55	0.62	0.49	0.61	0.67	-0.19	0.55	0.39	0.50	0.80	0.64	0.55
LOI											1.00	-0.48	-0.57	-0.74	-0.72	-0.67	-0.74	-0.74	0.15	-0.71	-0.65	-0.73	-0.27	-0.72	-0.63
Ba												1.00	0.29	0.25	0.23	0.24	0.23	0.22	-0.05	0.21	0.15	0.19	-0.21	0.23	0.13
Co													1.00	0.69	0.53	0.67	0.59	0.54	0.58	0.68	0.73	0.62	0.31	0.56	0.65
Cr														1.00	0.96	0.97	0.99	0.97	0.33	0.99	0.94	0.96	0.73	0.98	0.98
Hf															1.00	0.92	0.99	0.97	0.18	0.97	0.89	0.95	0.72	0.99	0.96
Ni																1.00	0.96	0.92	0.39	0.98	0.91	0.94	0.73	0.94	0.96
Rb																	1.00	0.99	0.23	0.99	0.91	0.97	0.74	0.99	0.98
Sc																		1.00	0.18	0.97	0.89	0.97	0.76	0.99	0.96
Sr																			1.00	0.34	0.45	0.25	0.32	0.20	0.37
Th																				1.00	0.93	0.97	0.76	0.98	0.99
U																					1.00	0.92	0.62	0.90	0.92
V																						1.00	0.67	0.96	0.95
Y																							1.00	0.76	0.79
Zr																								1.00	0.97
∑REE																									1.00

Calcium, magnesium, and manganese. The calcium content is ranged between 0.39 % - 14.16 % exactly opposite of the other major elements. It increases in section Q1 and decreases in section Q2. Calcium has a negative correlation coefficient with all elements except manganese and has a positive moderately strong (r = 0.54) and high correlation value with LOI (r = 0.97), which may confirm that the calcium is linked to the carbonate phase precipitated in synchronized with the radiolarian chert as very thin veins or strewn. The magnesium content is approximately equal in both sections, not exceeding 1% in general (Table 1). Magnesium has a positive strong correlation coefficient to many major elements such as aluminum, titanium, iron, sodium, and potassium (Table 3). The manganese contents are low in all samples of two sections and exceed 1 % in one sample, MgO ranges from 0.02 % to 0.13 %, and has a negative correlation to most major oxides except calcium and LOI has a positive correlation (r = 0.54) and (r = 0.97) respectively, which can indicate the secondary origin of manganese content as migration or substitute during the diagenetic processes (Halamic et al., 2005).

Table 4. Significance ratios of geochemical data in both sections.

Samples	**Section Q1**						**Section Q2**					
Variables	**Q11**	**Q12**	**Q13**	**Q14**	**Q15**	**Q16**	**Q21**	**Q22**	**Q23**	**Q24**	**Q25**	**Q26**
Si/(Si+Al+Fe+Ca)	0.87	0.85	0.83	0.84	0.94	0.91	0.84	0.83	0.85	0.85	0.84	0.84
CaO/(CaO+MgO)	0.89	0.99	0.97	0.98	0.99	0.61	0.35	0.31	0.28	0.32	0.33	0.28
Fe_2O_3/TiO_2	8.09	9.43	10.90	8.40	6.68	6.42	9.28	7.98	7.69	8.33	9.19	9.37
MnO_2/TiO_2	0.11	2.37	1.01	1.69	1.84	0.06	0.18	0.07	0.06	0.05	0.13	0.10
$(La/Ce)_n$	1.28	1.30	1.31	1.36	1.24	1.46	1.47	1.48	1.63	1.54	1.68	1.65
Eu/Eu*	0.63	0.91	0.74	0.82	0.00	0.75	0.63	0.91	0.79	0.93	1.03	0.73
Ce/Ce*	0.76	0.57	0.97	0.78	0.70	1.08	1.45	1.52	1.40	1.50	1.46	1.69
Al_2O_3/TiO_2	17.4	22.0	21.9	15.6	16.6	15.4	19.5	17.3	17.6	18.8	16.4	19.1
Al/(Al+Fe+Mn)	0.68	0.65	0.65	0.61	0.66	0.70	0.67	0.68	0.69	0.69	0.64	0.67
$Al_2O_3/(Al_2O_3+Fe_2O_3)$	0.68	0.70	0.67	0.65	0.71	0.71	0.68	0.68	0.70	0.69	0.64	0.67

4.2.2. Trace elements

There is a substantial difference between the two sections in the content of trace elements. This is well observed in the lack of trace elements in samples Q11-Q16 while these elements are enriched in samples Q21-Q26 (Table 5) which may reflect the difference in provenance or depositional environment. Murray (1994) suggests that the dilution of trace elements could take place by diagenetic processes during the accumulation of radiolarian chert and an additional contribution of silica from the clay and shale particles. The negative correlation of all trace elements (except barium) to SiO_2 (r = -0.29 to -0.78) that is shown in Table 3 supports the suggestion of Murray (1994). Barium shows a weak positive correlation with most major elements such as Si, Al, Ti, Fe, and Mg (Table 3) which can be attributed to their association with the clastic part (shale) so that barium and potassium are accompanied in a magmatic environment and separated geochemically by hydrothermal processes (Berner, 1973). The lithophile elements (Ba, Hf, Rb, Sc, Sr, Th, U, and Y) are transported in a suspended phase to the sedimentation basin and used as evidence of input material from terrigenous and as measurement criterion to distance between the continental margin and site of sedimentation. This is clearly shown by the difference in concentration of these trace elements in the two sections (Table 2). Strontium is not connected with carbonate fraction due to a very low correlation coefficient with calcium (r = 0.04) and magnesium (r = 0.07) but has relatively high correlated value to manganese (r = 0.63) which may reflect adsorption on manganese dioxide (δ-MnO_2) at high temperatures (Karaseva et al., 2019). The lithophile elements (Cr, V) and high field strength elements (Hf, Zr) often exist in resistant minerals but could be enriched in hydrothermal precipitation which promotes their detritus input from terrigenous source (Gundlach and Marchig, 1982). Chromium shows a strong positive correlation with hafnium, vanadium and zirconium (r = 0.96: r = 0.96: r = 0.98) respectively. Cobalt has a moderate positive correlation with nickel (r = 0.67) but has a strong correlation coefficient with aluminum, titanium, iron, magnesium sodium, and potassium (Table 3). Nickel is associated with iron in hydrothermal sources while magnesium and cobalt are compatible elements with high mobility during diagenetic processes, therefore, it should be interpreted carefully and cautiously because of multi-source and variable behavior. Scandium has various origins in sediments but mostly it comes from deep weathering of igneous rocks, the strong positive correlation with major elements such as Al, Ti, Fe, Mg, Na, and K, and trace elements like Cr, Hf, Ni, and Rb support this idea.

4.2.3. Rare earth elements

Rare Earth Elements (REEs) are less affected by the weathering processes, alteration, and metamorphism as well, their concentrations and distribution patterns are greatly affected by the sources and origin of these rocks. The total REEs concentration in both sections is less than their total content in the upper continental crust (U.C.C.) (Rudnick and Gao, 2003), world average shale (Piper, 1974), and Post-Archean Australian Shale (PAAS) (McLennan, 2001). The highest total REEs reached (141.3 ppm) in section Q2, while in section Q1, the highest total REEs (57.7 ppm) was much lower than their average in section Q2. The REE contained in chert can indicate the depositional environment, for example, the Ce anomaly can be used to estimate the relative distance from the terrigenous sediment source, Murray et al. (1990). Ce anomaly in chert has average values of 0.29 at a mid-oceanic ridge, 0.6 in an ocean basin, and 0.9–1.30 at a continental margin (Murray 1994). The Ce anomaly average (0.81) in section Q1 and (1.50) in section Q2, which means this section is closer to the continental margin, and the same case for the Eu anomaly (0.64) in section Q1 and (0.84) in the section Q2. Total REEs has a strong positive correlation coefficient ($r \geq 0.90$ to 0.99) with most major and trace elements like (Al, Ti. Fe, Mg, Na, K, Cr, Hf, Ni, Rb, Sc, Th, U, V, and Zr) (Table 3) which indicates their common origin that related to detritus components input in a sedimentation basin. The chondrite normalized (REEs) patterns in the studied radiolarian chert are characterized by (a negative slope pattern) in both sections, but there are basic differences, the first: is a positive cerium anomaly in section Q2 and a negative cerium anomaly in section Q1 (Fig. 4a), as well as negative europium anomaly in both sections. Secondly: enrichment of all REEs in section Q2 generally, in addition to the negative anomaly of thulium (Tm), that revolved in sample Q15, which is characterized by high silica content ($SiO_2 > 93$ %) and depletion in most REEs, that may negatively effect on their average content. In regard to the normalized to (PAAS) and (UCC), they are characterized by the flat pattern (Fig. 4b and c) with the same anomalies of cerium compared to the chondrite normalized pattern.

Table 5. Geochemical analysis of Rare Earth Elements (ppm) in the two sections.

Sample		**La**	**Ce**	**Pr**	**Nd**	**Sm**	**Eu**	**Gd**	**Tb**	**Dy**	**Ho**	**Er**	**Tm**	**Yb**	**Lu**	**∑REE**
Section Q1	Q11	12.0	19.0	3.1	12.1	2.7	0.5	2.2	0.4	1.8	0.3	0.8	0.1	0.9	0.1	56.0
	Q12	8.3	9.4	1.9	7.3	1.3	0.4	1.4	0.2	1.6	0.3	0.7	0.0	0.7	0.1	33.6
	Q13	8.7	17.1	2.1	8.0	1.6	0.4	1.7	0.2	1.3	0.3	0.7	0.1	0.5	0.1	42.8
	Q14	7.6	10.9	1.5	5.5	0.8	0.2	0.7	0.2	0.7	0.2	0.4	0.0	0.4	0.1	29.2
	Q15	2.2	2.7	0.4	1.6	0.3	0.0	0.2	0.0	0.2	0.0	0.1	0.0	0.0	0.0	7.70
	Q16	10.6	25.0	3.0	10.2	2.1	0.5	2.0	0.3	1.8	0.4	0.9	0.1	0.7	0.1	57.7
Section Q2	Q21	23.1	68.4	5.7	19.3	3.8	0.8	3.9	0.7	2.7	0.6	1.6	0.2	1.2	0.2	132.2
	Q22	24.5	75.2	5.9	19.9	4.3	1.1	3.2	0.6	3.0	0.6	1.4	0.2	1.2	0.2	141.3
	Q23	23.6	68.0	5.9	18.0	3.3	0.8	2.9	0.4	2.5	0.5	1.2	0.2	1.1	0.2	128.6
	Q24	21.8	65.7	5.2	16.8	2.9	0.8	2.4	0.4	2.0	0.4	1.1	0.2	1.1	0.1	120.9
	Q25	21.6	67.0	5.8	17.2	2.5	1.0	3.5	0.6	3.0	0.5	1.1	0.2	1.2	0.2	125.4
	Q26	23.5	79.5	5.6	16.9	4.1	0.8	2.7	0.4	2.6	0.4	1.3	0.2	1.2	0.1	139.4
		Q11	Q12	Q13	Q14	Q15	Q16	Ave.	Q21	Q22	Q23	Q24	Q25	Q26		Ave.
Eu/Eu*		0.63	0.91	0.74	0.82	0.00	0.75	0.64	0.63	0.91	0.79	0.93	1.03	0.73		0.84
Ce/Ce*		0.76	0.57	0.97	0.78	0.70	1.08	0.81	1.45	1.52	1.40	1.50	1.46	1.69		1.50

Ce/Ce* $=Ce_N/(La_N \times Pr_N)^{1/2}$ and **Eu/Eu*** $=Eu_N/(Sm_N \times Gd_N)^{1/2}$.

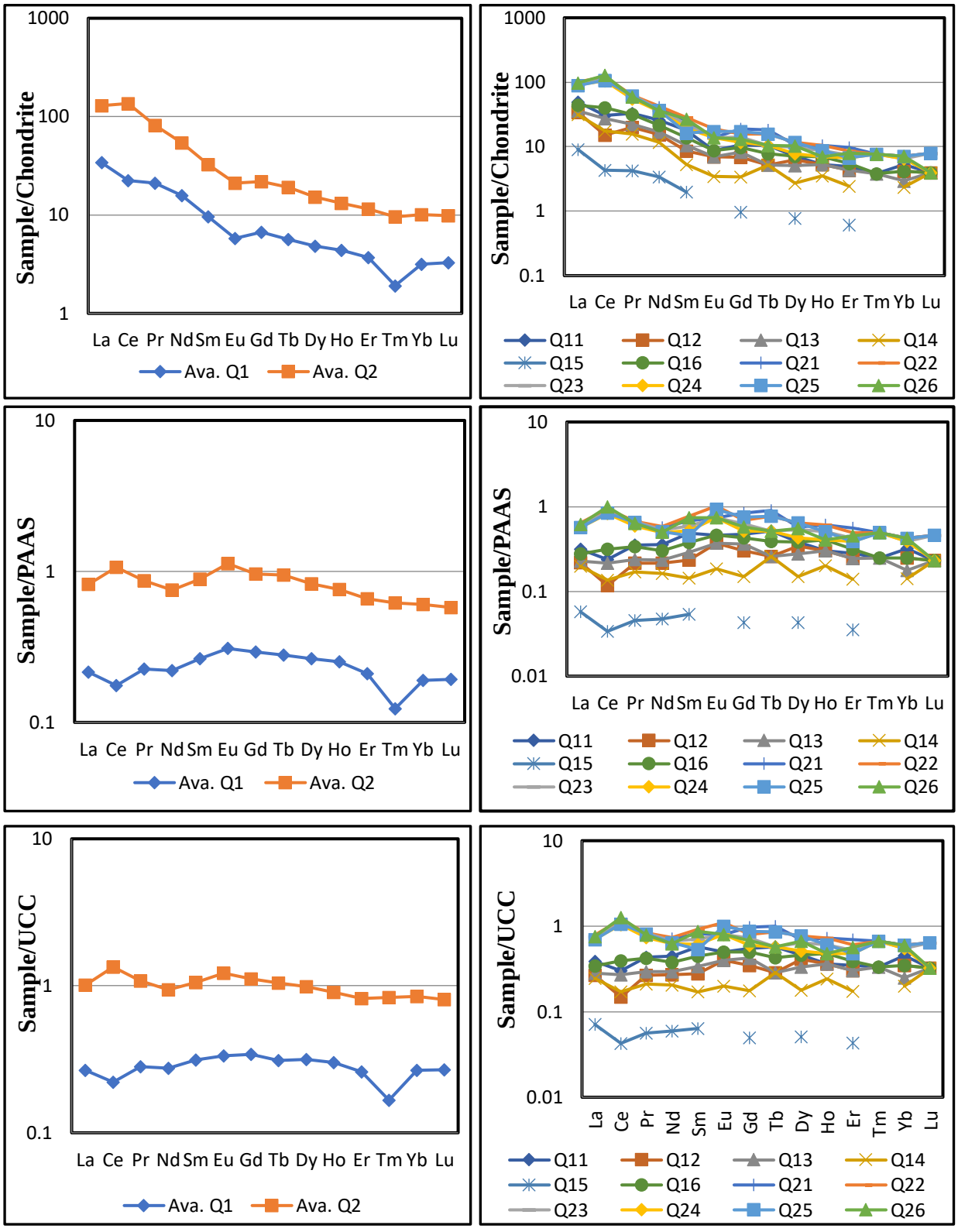

Fig. 4. Normalized REE patterns of the average and all samples in the two sections. a: Chondrite normalized (Sun and McDonough,1989); b: PAAS normalized (Mclennan, 2001); c: UCC normalized (Rudnick and Gao, 2003).

4.3. Provenance and Depositional Environment

In northeastern Iraq, ophiolite which represents the oceanic crust and commonly capped by radiolarian. In Penjween area the Cretaceous radiolarian chert (Qulqula Group) covers mafic and ultramafic igneous rocks (Al-Qayim et al., 2012). The Qulqula Formation is rich in silica and the Si/(Si+Al+Fe+Ca) ratio range from 0.83 to 0.94 which may indicate that the source of silica is the biogenic origin and with additional SiO_2 provided from shale fraction by diagenetic processes (Murray, 1994). Manganese is used as an indicator of the hydrothermal component while titanium represents terrigenous sources (Shimizu et al., 2001). The Al-Fe-Mn diagram (Fig. 5) (Adachi et al., 1986) shows that all samples fall into field (I) of non-hydrothermal zone whereas, in the SiO_2 vs Al_2O_3 diagram (Fig. 6), the samples of Q1 section fall into hydrothermal field and samples of Q2 section fall into non-hydrothermal field. The input materials in the Qulqula radiolarian chert come from terrigenous sediments in both sections as shown in (Fig. 7). On the other hand, the Al/(Al+Fe+Mn) ratio ranged between (0.61 to 0.70) which is very close to its values in average shale composite (0.6.19) which reflect the contribution of continental and non-hydrothermal sediments (Baltuck, 1982) while the lower values of this ratio reflected hydrothermal source input.

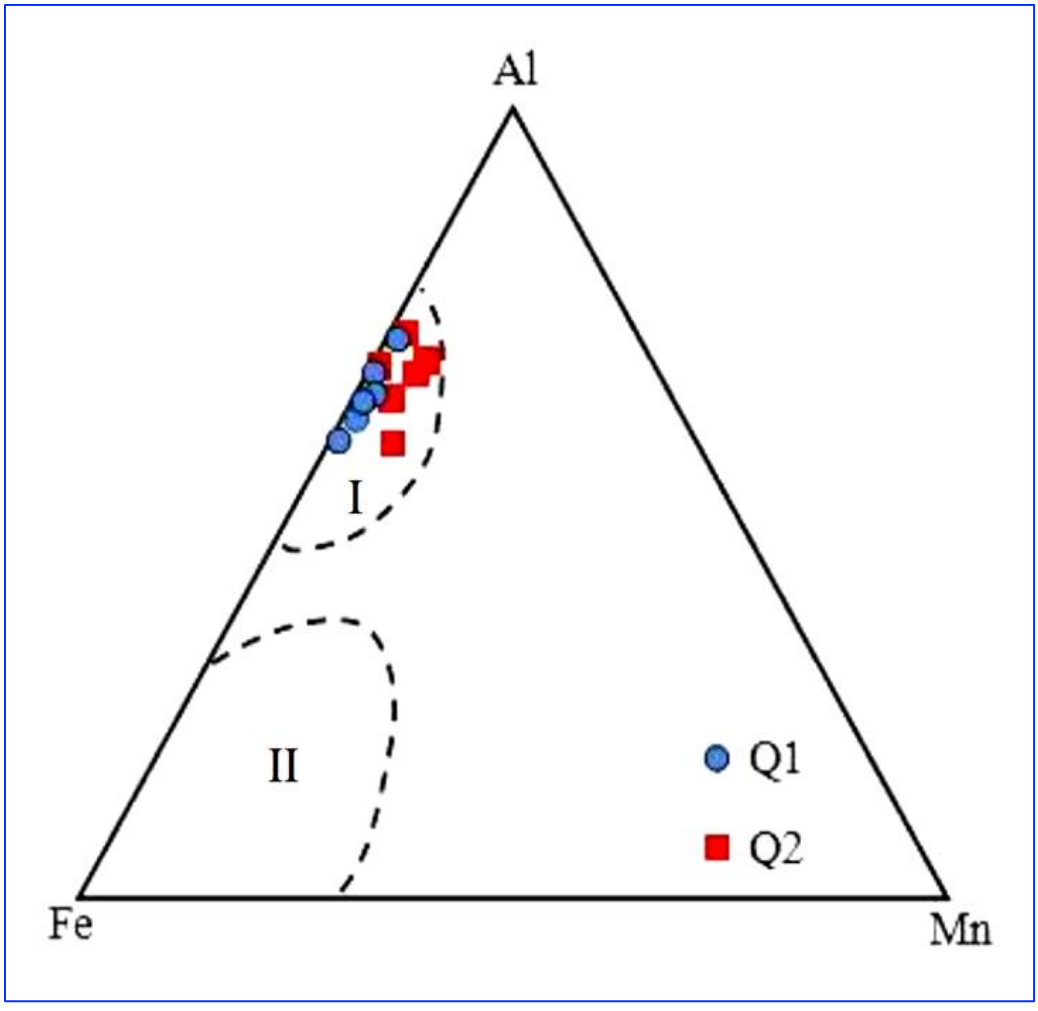

Fig. 5. Al-Fe-Mn diagram. Hydrothermal (II) and non-hydrothermal (I) fields after (Adachi et al., 1986).

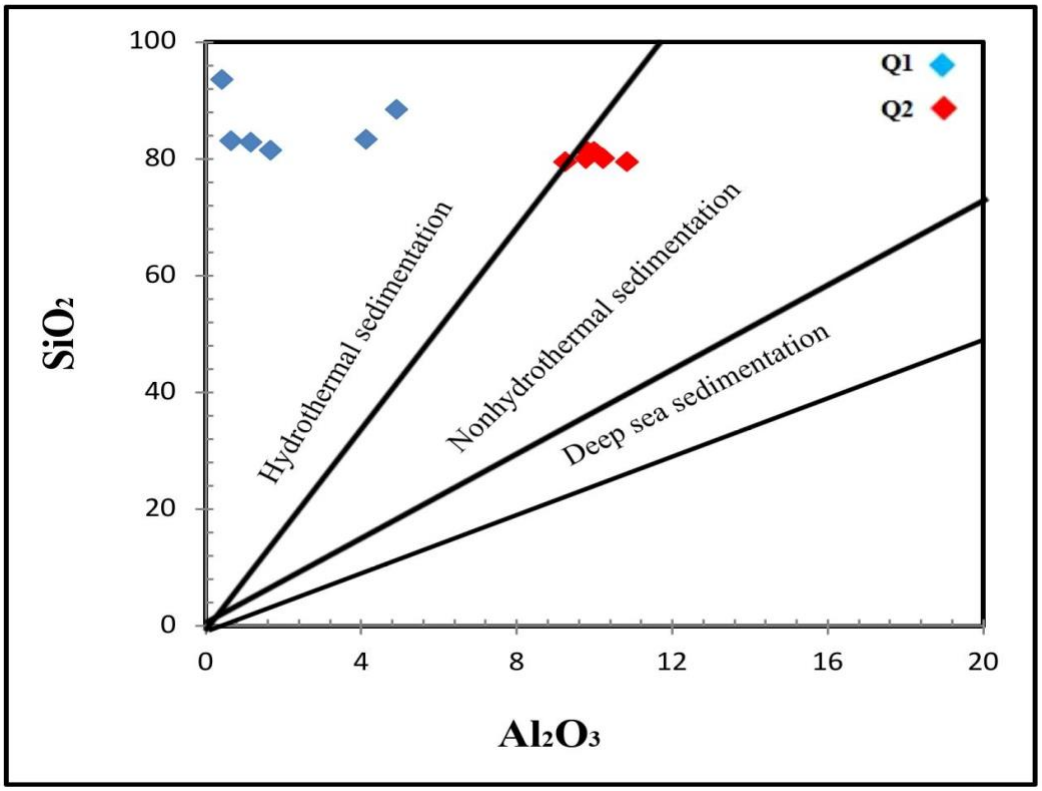

Fig. 6. Major oxides discrimination diagram (SiO_2 vs Al_2O_3) supporting hydrothermal and non-hydrothermal processes for the genesis of chert rocks, after (Crerar et al., 1982).

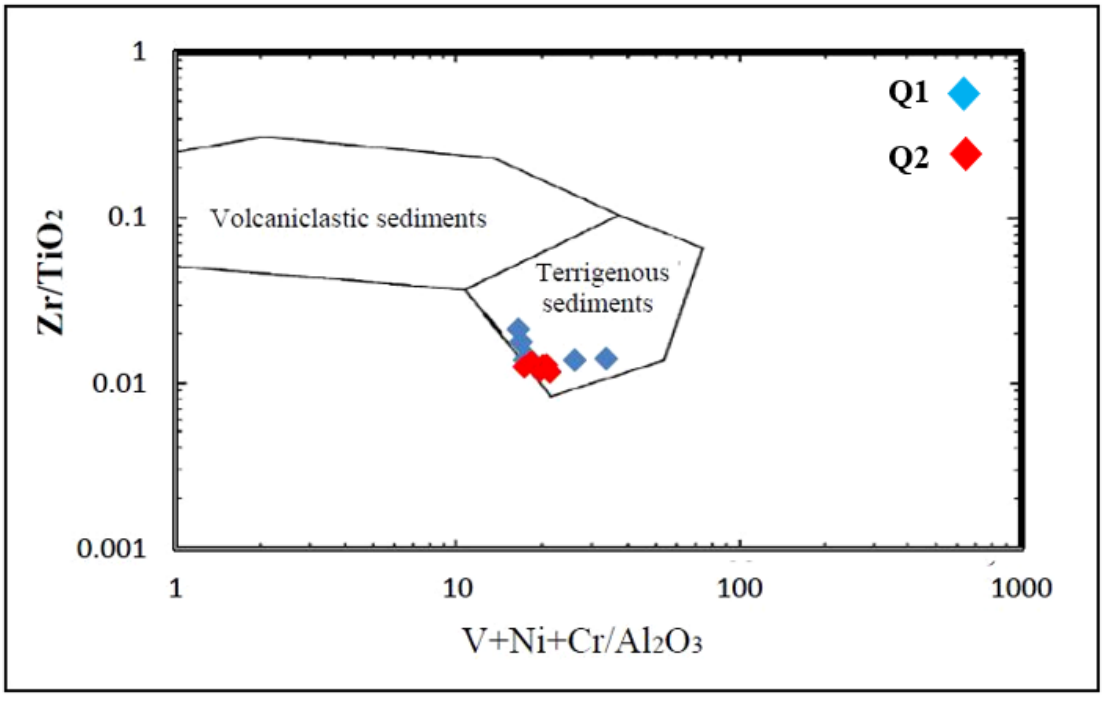

Fig. 7. Zr/TiO_2 vs. $V+Ni+Cr/Al_2O_3$ discrimination diagram of input materials origin for chert rocks, after (Andreozzi et al., 1997).

The radiolarian chert of the Qulqula Formation is deposited in two different environments as shown in Fig. 8, the samples of the Q1 section fall in the overlapping zone between the marginal sea (continental margin) and deep-sea environment while the samples of Q2 section falls in deep sea (pelagic) environment. Deposition of chert in a continental margin (marginal sea) environment with influence of terrigenous input requires $Al_2O_3/(Al_2O_3 + Fe_2O_3)$ ratios > 0.50 and Fe_2O_3/TiO_2 ratios < 50 (Liao et al, 2019). In marine sediments Ce anomaly can be used as an indicator of depositional environment, siliceous rocks show negative Ce anomaly at or near continental margin (Murray et al., 1990). In the Qulqula Formation, Ce appears negative anomaly in section Q1 and a positive anomaly in section Q2 (Fig. 4). which also promotes the deposition in two different environments.

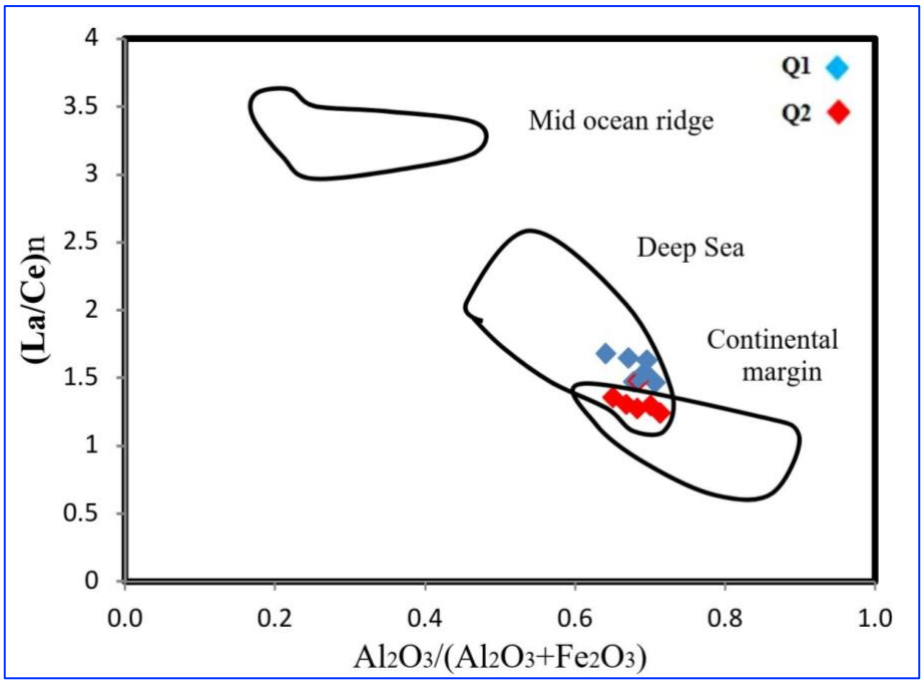

Fig. 8. Al_2O_3 / (Al_2O_3 + Fe_2O_3) vs (La / Ce) N diagram. Distribution samples in the depositional environment (mid-oceanic, Deep sea, and continental margin), after (Murray, 1994).

The chemical composition supports the idea that the Qulqula Formation are formed into two different environments, deep sea and continental margin. (Dasgupta et al., 1999) noted if the CaO/(CaO+MgO) ratio > 0.70 is characteristic for the freshwater environment, while this ratio < 0.50 is characteristic for the saline water environment. The CaO/(CaO+MgO) ratio in the present study range between 0.28 to 0.99 and decrease from sample Q11 to sample Q26 (Table 4) which indicates the deposition of the Qulqula radiolarian chert in the continental margin and deep sea (pelagic) environments. According to MnO_2/TiO_2 ratio, the Qulqula Formation can be divided into two groups, the first group has values ranging between 0.06 to 2.37 and the second group has values ranging from 0.04 to 0.18 (Table 4). Kunimaru et al., (1998) and Shimizu et al., (2001) considered that the values MnO_2/TiO_2 ratios < 0.50 is an index to continental shelf, continental slope, continental margin setting, and environments near basaltic islands while the values more than 0.50 a typical characteristic for the deep ocean, trenches, and basaltic plateau sediments.

5. Conclusions

The current study comprises a comprehensive geochemical analysis of radiolarian chert rocks in two sections in the Penjween area, focusing on the importance of geochemical data for tracking the rock sources and sedimentary environments. Diagrams and geochemical investigations have established that there is a fundamental difference between the two sections. The following are the main concluding remarks:

- The Si/(Si+Al+Fe+Ca) ratio range (0.8 – 0.94) may indicate that the silica source is of biogenic origin with the contribution of SiO_2 from shale fraction by diagenetic processes.
- Aluminum and titanium concentrations signify the terrigenous source materials such as mica and clay minerals due to a strong correlation to aluminosilicates, and their higher concentration in Nalparez Q2 section compared to Dolasur Q1 section indicate the continental margin setting.
- The relatively high concentration of phosphorous in section Q2 suggests that this section closer to the mid-oceanic ridge and sedimentation environment was affected by volcanic activities and diagenetic processes because of the association of chert to ophiolitic rocks.
- Lithophile elements (Cr, V) and high field strength elements (Hf, Zr) often exist in resistant minerals but could be enriched in hydrothermal precipitation, and the elements (Ba, Hf, Rb, Sc, Sr, Th, U, and Y) are transported as a suspended phase to the sedimentation basin
- Chondrite normalized (REEs) patterns in the radiolarian chert are characterized by (a negative slope pattern) in both sections, but the basic difference is a positive cerium anomaly in section Nalparez Q2 and a negative cerium anomaly in section Dolasur Q1 Negative Ce anomaly means that depositional environment at or near the continental margin.
- The Al-Fe-Mn diagram shows that all samples fall into field (I) “non-hydrothermal zone” but in SiO_2 vs Al_2O_3 diagram the samples of (Dolasur Q1) section fall into the hydrothermal field and samples of Nalparez Q2 section fall into non-hydrothermal field. On the other hand, the Al/(Al+Fe+Mn) ratio ranges between (0.61 to 0.70) which is very close to its values in average shale composite (0.6.19) which may reflect the contribution of continental and non-hydrothermal sediments.
- (Ln/Ce) n Vs $Al_2O_3/(Al_2O_3 + Fe_2O_3)$ diagram shows that the Qulqula Formation was deposited in two different environments, the samples of Dolasur Q1 section fall in the overlapping zone between the marginal sea (continental margin) and deep sea environment while the samples of (Nalparez Q2) section falls in deep sea (pelagic) environment.
- The chemical composition of the Qulqula chert supports the idea that the two sections are formed into two different environments, “deep sea and continental margin”, because the CaO/(CaO+MgO) ratio > 0.70 is characteristic of the freshwater environment (Dolasur Q1) section, while this ratio < 0.50 is characteristic for the saline water environment (Nalparez Q2) section.
- According to MnO_2/TiO_2 ratio the Qulqula Formation can be divided into two groups, the first group has values ranging between 0.06 to 2.37 which is a typical characteristic of the deep ocean, trenches, and basaltic plateau sediments. and the second group has values ranging between 0.04 to 0.18 pointing to continental shelf, continental slope, continental margin, and environments near basaltic islands.
- Finally, the Qulqula radiolarian chert is associated with ophiolite rocks and was deposited along the sedimentary basin starting from the continental margin through the deep open sea and was directly or indirectly affected by submarine volcanoes and hydrothermal solutions since section Q1 in the Dolasur village is closer to the open sea and may reach the mid-ocean ridge in other locations.

Acknowledgements

The authors thank Dr. Khalid J. A. and Dr. Azzam H. M. Al-Samman for their help during fieldwork in the Penjween area. We would also like to thank the Head of the Department of the Geology, University of Mosul for the immense support and help during working in the laboratories.

References

Adachi, M. Yamamoto K. and Sugisaki R., 1986. Hydrothermal chert and associated siliceous rocks from the northern Pacific: their geological significance as indicator of ocean ridge activity. Sedimentary Geology, 47(1-2), 125-148

Ali, S., Mohajjel, M., Aswad, K., Ismail, S., Buckman, S. & Jones, B. (2014). Tectono-stratigraphy and structure of the northwestern Zagros collision zone across the Iraq-Iran border. Journal of Environment and Earth Science, 4 (4), 92-110.

Al-Kadhimi, J.A.M., Sissakian, V.K. Fattah A.S. and Deikran D.B. (1996). Tectonic Map of Iraq, State Company of Geological survey and Mining, Baghdad.

Al-Qayim, B. Omer, A. and Koyi, H. (2012). Tectonostratigraphic overview of the Zagros Suture Zone, Kurdistan Region, Northeast Iraq. GeoArabia, 17(4), 109-156

Andreozzi, M., Dinelli, E. And Tateo, F. (1997). Geochemical and mineralogical criteria for the identification of ash layers in the stratigraphic framework of a foredeep, the early Miocene Mt. Cervarola Sandstone, northern Italy. Chemical Geology, 137(1-2), 23-39.

Aswad, K.J.,1999. Arc-continent collision in northeastern Iraq as evidenced by Mawat and Penjween ophiolite complexes. Journal of Science, 10, 51- 61

Baltuck M., 1982. Provenance and distribution of tethyan pelagic and hemipelagic siliceous sediments, Pindos Mountains, Greece. Sedimentary Geology, 31, 63-88.

Bellen, R.C., Van Dunnigton, H.V., Wetzel, R., Morton, D.M., (1959). Lexique Stratigraphique International. V. III, Paris, 333.

Berner, R. A., 1973. Phosphate removal from seawater by adsorption on volcanogenic ferric oxides. Earth Planet, 18, 77–86

Bolton, C.M.G., 1955. Report on the Geology and economic prospects of the Qalat Dizeh area, Site Investment Co. Ltd. Report no. 32, D.G. Geological Survey and Mineral Investigation Library, Baghdad, 139-160.

Bolton, C.M.G.,1958. Geological map-Kurdistan series, scale 1:100,000 sheet K4, Rania, Site Investment, Co. Ltd. Report, 36, D.G. Geological Survey and Mineral Investigation Report no. 276.

Bragin, N. Ledneva, G. Bragina, L. Tsiolakis E. Symeou V. and Papadimitriou, N., 2022. The radiolarian age and petrographic composition of a block of the Lower Jurassic volcaniclastic breccia and chert of the Mamonia Complex, SW Cyprus, 75(1), 115–128.

Buday, T., 1980. The Regional Geology of Iraq, vol I, Stratigraphy and Paleogeography. Kassab, I.I. and Jassim, S.Z., Eds., GEOSURV, Baghdad, 445.

Buday, T., Jassim, S. Z., 1987. The Regional Geology of Iraq, vol. II: Tectonism, Magmatism and Metamorphism. Publication of GEOSURV, Baghdad, 352.

Crerar, D. A., Namson, J., Chyi, M., Williams, L. and Feigenson, M. D., 1982. Manganiferous cherts of the Franciscan assemblage; General geology, ancient and modern analogues, and implications for hydrothermal convection at oceanic spreading centers. Economic Geology, 77 (3), 519–540.

Dasgupta, H. C., Sambasiva, V. V. And Krishna C., 1999. Chemical environments of deposition of ancient iron- and manganese-rich sediments and cherts. Sedimentary Geology, 125 (1), 83-98.

Dunham, R. J., 1962. Classification of carbonate rocks according to depositional texture: in Ham, W. E. (ed.), Classification of rocks: a symposium, American Association of Petroleum Geologist, 1, 108-121.

Gharib, F. And De Weaver, P., 2010. Radiolaires mésozoïques de la formation de Kermanshah (Iran). Comptes Rendus Palevol, 9 (5), 209-219.

Gundlach, H., and Marchig V., 1982. Ocean floor "Metalliferous sediments" two possibilities for genesis. In: Halamic J., Marchig V., and Gorican S. 2005, Jurassic radiolarian cherts in north-western Croatia: Geochemistry, material provenance and depositional environment. Geologica Carpathica, 56(2), 123 – 136.

Halamic, J., Marchig, V., and Gorican, S. (2005). Jurassic radiolarian cherts in north-western Croatia: Geochemistry, material provenance and depositional environment. Geologica Carpathica, 56(2), 123 – 136.

Jassim, S.Z. and Goff, J.C., 2006. Geology of Iraq. Published by Dolin, Prague and Moravian Museum, Brno, 34.

Karaseva, O. N., Ivanova, L. I. and Lakshtova, L. Z., 2019. Strontium adsorption on manganese oxide (δ-MnO2) at elevated temperatures: experiment and modelling. Geochemistry International. 57, 1107–1119.

Karim, K. H., Habib, R. and Sardar, M. Raza, 2009. Lithology of the Lower Part of Qulqula Radiolarian Formation (Early Cretaceous), Kurdistan Region, NE Iraq University of Sulaimani, Iraqi Bulletin of Geology and Mining, 5(1), 9-23

Kunimaru, T., Shimizu, H., Takahasi, K., Yabuki, S., 1998. Differences in geochemical features between Permian and Triassic cherts from the Southern Chichibu terrane, southwest Japan: REE abundances, major element compositions and Sr isotopic ratios. Sedimentary Geology, 119, 195–217.

Liao, Z.W., Hu, W.X., Fu., X.G. and Hu, Z.Y., 2019. Geochemistry of upper Permian siliceous rocks from the Lower Yangtze region, south-eastern China: implications for the origin of chert and Permian ocean chemistry. Petroleum Science, 16, 252–266

McLennan, S. M., 2001. Relationships between the Trace Element Composition of Sedimentary Rocks and Upper Continental Crust, Geochemistry Geophysics Geosystems, 2(4), 1-24.

Murray, R. W., 1994. Chemical criteria to identify the depositional environment of chert: general principles and applications, Sedimentary Geology, 90(3-4), 213–232.

Murray, R. W., Buchholtz ten Brink, M. R., Gerlach, D. C., Russ, G. P., and Jones, D. L., 1992. Interoceanic variation in the rare earth, major, and trace element depositional chemistry of chert: Perspectives gained from the DSDP and ODP record. Geochimica et Cosmochimica Acta, 56(5), 1897-1913.

Murray, R.W., Buchholtz ten Brink, M. R., Jones, D. L., Gerlach, D. C., and Russ, P. G., 1990. Rare earth elements as indicators of different marine depositional environments in chert and shale, Geology, 18(3), 268.

Piper, D. Z., 1974. Rare-Earth Elements in the Sedimentary Cycle: A Summary. Chemical Geology, 14(4), 285-304.

Rangin, C, Steinberg, M, Bonnot-Courtois, C., 1981.Geochemistry of the Mesozoic bedded cherts of central Baja California (Vizcaino-Cedros-San Benito): Implications for paleogeographic reconstruction of an old oceanic basin. Earth and Planetary Science Letters, 54, 313–322.

Rudnick, R. L. and Gao, S., 2003. Composition of the Continental Crust, In: H. D. Holland and K. K. Turekian, Eds., Treatise on Geochemistry, Elsevier, New York, 1-64.

Ruitz-Ortiz, P.A., Bustillo, M.A. & Moliana, J.M., 1989. Radiolarite sequences of the Subbetic, Betic Cordillera, Southern Spain. In: HEIN, J.R. & OBRADOVIĆ, J. (eds): Siliceous deposits of the Tethys and Pacific regions. Springer Verlag, New York, 107-127.

Shimizu, H., Kunimaru, T., Yoneda, S., and Adachi, M., 2001. Sources and depositional environments of some Permian and Triassic Cherts: Significance of Rb-Sr and Sm-Nd isotopic and REE abundance data. The Journal of Geology 109(1):105-125

Sun, S. S., and McDonough, W. F. 1989. Chemical and isotopic systematics of ocean basalts: Implications for mantle composition and processes, in Magmatism in the Ocean Basins. Geological Society London Special Publications, 42, 313-345.